Indian Journal of Pure & Applied Physics
Vol. 47, September 2009, pp. 643-647

Surface morphological, band and lattice structural studies of cellulosic fiber coir under mercerization by ESCA, IR and XRD techniques

D N Mahato*, R N Prasad** & B K Mathur

Department of Physics, IIT, Kharagpur 721 301

*P G Department of Physics, Tata College, Chaibasa 833 202

** Department of Physics, J L N College, Chakradharpur

E-mail: dn.mahato08@yahoo.com

Received 4 March 2009; revised 29 May 2009; accepted 20 July 2009

The electron spectroscopy for chemical analysis (ESCA) studies show the increased binding energy (BE) of C_{1s} and O_{1s} on mercerization. The oxygen to carbon ratio increases. The cellulose I lattice structure is preserved, which is reflected in the XRD and IR spectra. These assume significance because these changes reflect in the structure-sensitive physical properties. The change in oxidation state is supported by 2929 cm^{-1} band. The band at 1267 cm^{-1} gives depolymerization. The IR band at 1433 cm^{-1} gives idea of restriction of lattice transformation from cellulose I into cellulose II, which is confirmed by XRD pattern. The fiber undergoes disappearance of crystallinity, depolymerization and oxidation.

Keywords: Electron spectroscopy, Chemical analysis, ESCA, XRD, IR, Crystallinity, Oxidation, Depolymerization, Lattice transformation

1 Introduction

Coir is a multicellular biopolymer in which crystalline cellulose is arranged helically in a matrix consisting of non-crystalline ligno-cellulosic complex[1]. Coir fiber is abundantly available in Southern India and tropics. Natural fibers are drawing greater attention than the artificially man made fibers from energy and ecological considerations. The fibers being light and good tenacity are finding use against the metals for bodies of automobiles[2]. The natural fibers reinforced polymer composites are finding use as textile and rubber composites[3-4]. The protective and attractive covering of a vegetated embankment using coir geotextiles has been successfully used by Vishnudas *et al*[5].

Coir fiber can be used as geotextiles for soil and water conservation[6-7]. Coir technology is being developed for civil engineering applications for low cost housing[7]. Coir cement composites are used to save energy consumption of buildings[8]. High amount of lignin and cellulose increases the strength of the composites. Coir boards compared to other commercial boards are light weight composites of low thermal conductivity. These fibers have low electrical conductivity[9] and are extremely important for energy saving with use as ceiling and wall material. The important physical properties such as mechanical, electrical and thermal are structure-sensitive. Coir fiber is a ligno-cellulosic complex. The structure of cellulose is very complex undergoing lattice transformation into various polymorphic forms under NaOH treatment, known as mercerization and this becomes more complex due to the presence of lignin and hemicellulose. Fiber-polymer and fiber-metal complex are formed for solving housing, textiles, domestic and commercial problems.

Cellulose, a fibrous polymer, forms large molecules mostly in the form of long chains. When these long chains under suitable conditions grow side by side in a regular way and at regular intervals they form crystals. However, the regularity in atomic arrangements in natural fibrous polymers have neither a perfection as observed in crystal Fig. 1(a) nor an extent of imperfection as in amorphous substance Fig. 1(d). The lattice defect, distortion depending upon the state of order existing in the lattice, are characterized as distortion of the first kind (type I) and distortion of the second kind (type II). In lattice, affected by type I distortions, the long range order are preserved Fig. 1(b). The magnitude of the displacement of atoms, groups of atoms or molecules from their positions in an ideal lattice is independent of the location in the crystal. In the distortion of the second kind Fig. 1(c), the magnitude of the displacements of atoms, group of atoms or molecules from their ideal lattice sites increase with the distance

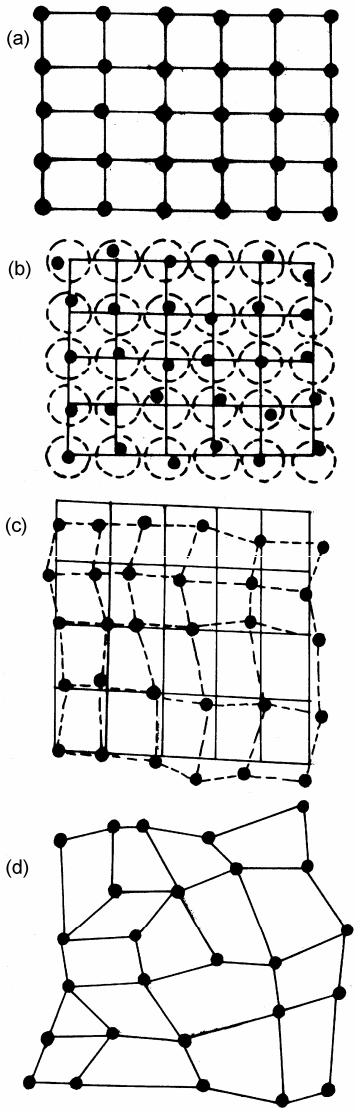

Fig. 1 — Lattice structures of cellulose (a) Perfect (undistorted) lattice, (b) Lattice distortions of the first kind, (c) Lattice distortions of the second kind and (d) Amorphous structure (no lattice)

from any arbitrary chosen reference point and long range order is not present. Such states have been described by various researchers as paracrystalline, which are characterized by a special type of distortion called type II, where long range order is not present. Based on numerous X-ray and electron microscopic studies and also on various models proposed to fit the experimental data, the fibrous polymers are believed to be in mixed state composed of crystalline, amorphous and paracrystalline phase[10-14].

Clark[15] first used X-ray photoelectron spectroscopic (XPS) technique known as ESCA to characterize celluloses and had predicted the presence of extraneous hydrocarbon adhering to the surfaces of the cellulose fibrils. Hence any attempt to interpret the X-ray diffraction data of cellulose in the light of existing models[10-14] needs a further consideration for the contributions arising out of these extraneous hydrocarbons. Li *et al*.[15] have studied the polymers by ESCA and IR techniques. Surface morphological ESCA study of ligno-cellulosic wood fiber has been made by Hon *et al*[16].

ESCA is very much useful for surface morphological studies up to the depth of 100Å because coating, finishing and adhesives are used on this portion of the material. Bond formations and dissociations among the chemical groups are associated with the change in BE of the orbital electrons, which are made by ESCA studies.

Infrared Spectroscopy has been used successfully by physicists and chemists to resolve problems of structural arrangements of organic and inorganic substances because the variations in infrared spectra of minerals are indicative of changes in symmetry of the molecules. This provides a versatile method for analyzing mineral structures at the molecular level. Transitions in structure are well recorded in IR. For the preparation of fiber-cement, fiber-metal or fiber-polymer composite, the characterization of the fiber in terms of lattice and band structure, defect and strain profile, crystallite size and packing configuration are essential. The binding energy (BE) and oxidation states known as chemical shifts are also essential. In this paper, lattice defects and particle size are studied by XRD, which dictate conditions conducive for composite formation. The band structure is studied by IR and chemical shifts are studied by ESCA. The binding energy is indirectly related to the mechanical strength of the fiber.

2 Experimental Details

Bristle ratted coir fibers were obtained by courtesy of Central Coir Research Institute, Allepey, Kerala, India. Fine uniform fibers were separated out and impurities from the surface were removed by gently rubbing the surface followed by prolonged washing with distilled water and drying. The fibers were treated with 5, 10, 15, 20 and 30% (w/w) of NaOH solution, respectively for 3h each. Some fibers were thoroughly washed with distilled water to remove alkali completely to get mercerized samples. To get soda-cellulose samples, the NaOH treated fibers were dried without washing and the excess of alkali was removed by gently pressing the surface of the fibers. The treated fibers were made powder of 200 mesh size by prolong grinding and sieving.

XRD diffractograms of the samples were recorded on a Philips X-ray diffractometer (PW1710) in the angular range 5°(2θ) to 90°(2θ) using filtered CuK_α radiation at 35 kV and 30 mA. IR spectra were taken by using Perkin Elmer Spectrometer at a resolution of 2.4 cm^{-1} with filter –2 and noise level –4.

ESCA measurements on coir fiber were performed on a VG Scientific ESCA LAB operating at a pressure of 1×10^{-8} torr with AlK_α radiation (1486.6 eV). Each specimen was analyzed for s-orbital BE of carbon, oxygen and sodium i.e., C_{1s}, O_{1s} and Na_{1s} peaks, respectively. Gold $4f_{7/2}$ level was used for calibration of the energy scale and the resolution under the experimental condition was of the order of 0.3 eV.

3 Results and Discussion

The high resolution core level spectra were smoothened using the Fourier series expansion. The overlapped peaks were resolved from knowledge of component peak positions and assuming them to be of Gaussian type[17].

The C_{1s} and O_{1s} spectra of raw coir and mercerized are shown in Figs 2 and 3, respectively. The C_{1s} spectra of coir fiber show three distinct components. The component of pure cellulose at 285.5 eV arises from the extraneous hydrocarbon, which is confined to the surface of the sample as reported by Clark[18]. The central component at 287.0 eV arises from the C_2, C_3, C_4, C_5 and C_6 carbon attached to one oxygen each. The C_1 attached to two oxygen gives the peak having the binding energy 288.5 eV. Hon[16] has found in the wood, which is a ligno-cellulosic complex the carbon-carbon or carbon- hydrogen binding energy 285.0 eV, the carbon attached to one oxygen atom –C–O– at 287.0 eV and carbon attached to two oxygen atoms –O–C–O– or –C=O at 289.5 eV. In the present study, the unresolved C_{1s} profile has peak at 291 eV and the resolved peaks are at 287.5, 290 and 292 eV, respectively. The coir fiber is a ligno-cellulosic complex like wood fiber but coir fiber has more lignin content. The composition of wood is cellulose 43%, hemicelluse 38% and lignin 20% approximately whereas in the coir fiber cellulose 46%, lignin 45%, hemicellulose 0.3% and other soluble materials. The shifting of the binding energy to the higher value may be due to the higher lignin content in the coir fiber. Because of cellulose chemical structure, namely, carbon bonded to carbon and to oxygen, it can account for C_1 and C_2 peaks. C_3 peak is due to hemiacetal linkage. In principle, cellulose has the

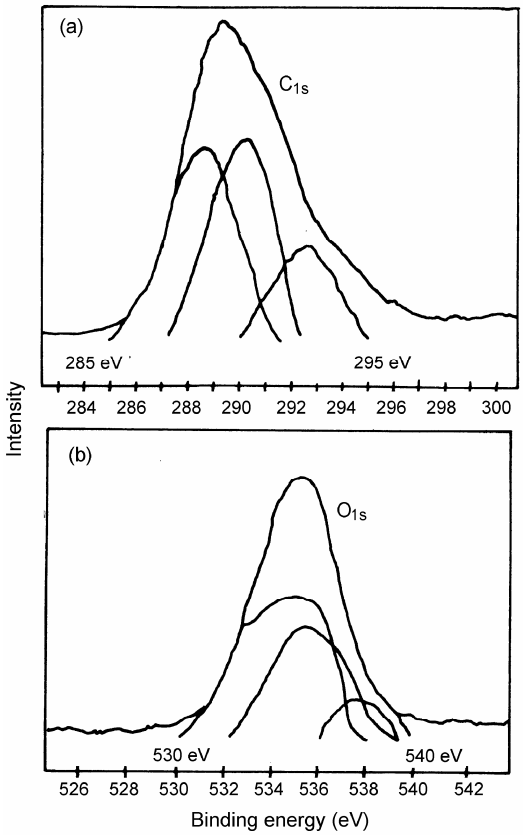

Fig. 2 — Binding energy (BE) of (a) C_{1S} of the raw fiber, (b) O_{1s} of the raw fiber

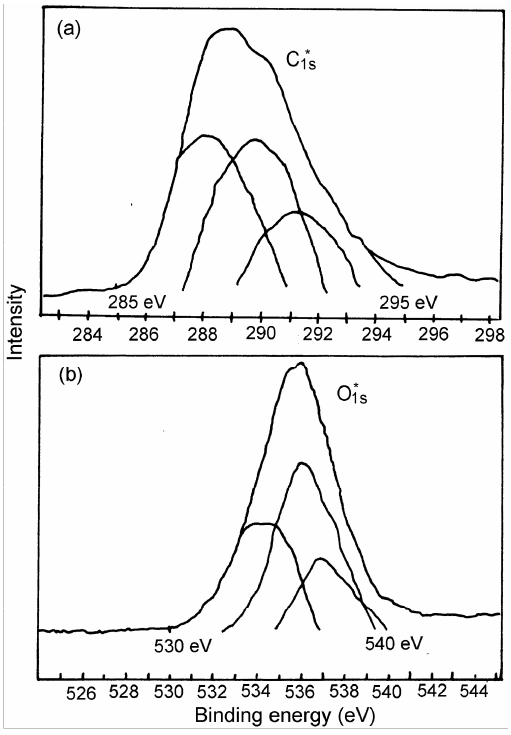

Fig. 3 — Binding energy (BE) of (a) C^*_{1S} of the 20% mercerized fiber; (b) O^*_{1S} of the 20% mercerized fiber

gross formula ($C_6H_{10}O_5$) and thus oxygen-to-carbon ratio should be 0.83. However, the ESCA experimental data shows unsatisfactorily low oxygen-to-carbon ratio value, i.e. 0.77. This implies that impurities with hydrocarbon nature are possibly deposited at the cellulose surface. The oxygen-to-carbon ratio in lignin is 0.34. From the oxygen-to-carbon ratio, which is obtained from the area of the ESCA profiles, it is apparent that the fiber surface is relatively high in carbon-to-carbon (C–C) and carbon-to-hydrogen (C–H) bondings, which is characteristically hydrophobic in nature. The same surface characteristics is for lignin. But cellulose is high in oxygen-to-carbon bondings, i.e. more hydrophilic in nature. The lignin is an aromatic compound, which also contributes to the C_{1s} peak.

In the raw sample of coir fiber, the deconvoluted Gaussian profiles have peak positions in the C_1, C_2 and C_3 at 288.4, 290.3 and 292.0 eV, respectively. In the raw sample, peak positions of O_1, O_2 and O_3 are at 535.0, 535.3 and 537.9 eV, respectively. The ratio of carbon- to- oxygen which is given by the ratio of two curves stands at 0.77.

In the 20% mercerized sample of coir fiber, the peak positions of C_1*, C_2* and C_3* are at 287.5, 290.0 and 292.0 eV, respectively. It is obvious that the carbon atoms on the surface are affected first by the mercerization, decreasing the binding energy of C_1*, the binding energy of C_2* and C_3* also decreased marginally but the individual profile areas increase, which indicates the increased BE and mechanical strength of the fiber[19].

The peak positions of the O_1*, O_2* and O_3* of the 20% mercerized sample are at 533.5, 536.6 and 537.4 eV, respectively. In the 20% mercerized sample the oxygen-to-carbon ratio is 0.86. This is quite obvious that mercerization is accompanied by oxidation. The irregular change in the binding energy of oxygen is due to the complex structure of ligno-cellulosic fiber, which is further complicated by mercerization. The elemental analysis also shows a significant increase in the percentage of oxygen on mercerization[20].

ESCA results may be corroborated by IR studies shown in Fig. 4. The IR band at 2929 cm^{-1} is assigned to CH_2 anti-symmetric stretching[21]. In the 20% mercerized fiber the band shifts to lower frequency side at 2905 cm^{-1}. The total intensity of the band, which can be measured by the absorption band area, decreases with mercerization, which concludes that carbon atoms attached to carbon or hydrogen (–C–C– or –C–H) decrease.

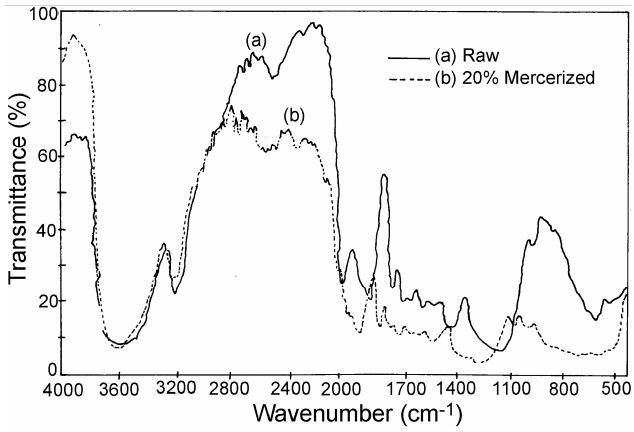

Fig. 4 — Overlapped IR spectra of the raw and 20% mercerized fiber

1735 cm^{-1} Band — This band is attributed to C=O stretching of the carbonyl and acetyl groups in the 4-O-methyl-glucuronoacetyl xylan component of hemicellulose in coir fiber. This band interestingly disappears on mercerization.

1607 cm^{-1} Band — This band is attributed to the molecular vibration of adsorbed water molecules. The intensity of this band increases on mercerization.

1508 cm^{-1} Band — This is the presence of aromatic rings of lignin, which decreases in intensity on mercerization.

1267 cm^{-1} Band — This band is assigned to –C–O–C– bond in the cellulose chain[22]. This broad medium band shifts to 1268 cm^{-1} and becomes very weak broad band on 20% mercerization. This may be due to depolymerization by alkali treatment.

1433 cm^{-1} Band — This band is assigned to the CH_2 symmetrical deformation[23-24] and on 20% mercerization shifts to low frequency 1425 cm^{-1} without any significant change in the intensity of band. The effect of change of this band is related to the change in the environment of the C_6 carbon atom due to formation or breaking of the hydrogen bond involving the atom O_6.

This indicates the change in lattice from cellulose I into cellulose II. The lattice transformation from cellulose I into cellulose II is restricted due to the presence of lignin[25]. Since in the case of lattice transformation the intensity of this band change significantly, which is not taking place here.

The XRD pattern of raw fiber and 20% mercerized coir fiber have been shown in Fig. 5. It is quite obvious that the crystallinity decreases on 20% mercerization involving depolymerization, which is evidenced by the decrease in the intensity of

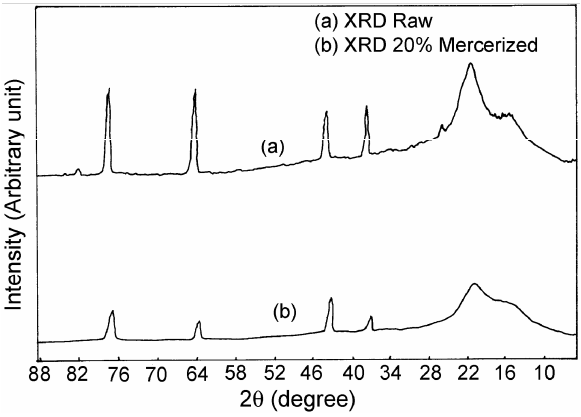

Fig. 5—XRD pattern of the raw and 20% mercerized fiber

absorption band at 1267 cm^{-1} and by electron scanning microscopy (SEM) grain size[20]. But the lattice transformation from cellulose I into cellulose II is restricted due to the reason mentioned above[25].

The native cellulose I and the regenerated cellulose II lattice on mercerization have distinct XRD patterns due to parallel chain arrangements confirming model calculations[26]. That change in the XRD pattern is not observed here.

References

1 Ott E, Spurlin H M & Graffin M W, (eds) *Cellulose and cellulose derivatives,* Part II (Interscience, New York) 1954, pp 863.

2 Al-Quereshi HA, *2nd International Wood and Natural Composites Symposium*, Kassel/Germany, 28-29 June 1999.

3 Singh B, Gupta M & Verma A*, Polym Composites,* (Brook field), 17 (1996) 910.

4 Vargheese S, Kuriakose B & Thomas S, *J Appl Polym Sci*, 53 (1994) 1051.

5 Vishnudas S, Savenije H H G, Zaag P Van der, Anil K R & Balan K Hydrol, *Earth Syst Sci*, 10 (2006) 565.

6 Amit K R & Sebastian R, Effect of Coir Geotextiles in Soil Conservation and slope land cultivation in Varying land slopes with forest loam soil, in: *Case histories of geosynthetics in infrastructure*, edited by Mathur G N, Rao G V & Chawla A S (CBIP publications, N. Delhi), 2003.

7 Balan K , Case studies on the civil Engineering Applications of Coir Geotextiles, in: *case histories of geosynthetics in infrastructure*, edited by Mathur G N, Rao G V & Chawla A S, (CBIP publications, N Delhi) , 2003, pp 172.

8 Asasutjarit C, Hirunlabh J, Khedari J, Daguenet M, Quenard D & Kmutt, *BSRC 10DBMC International Conference on Durability of Building Materials and Components* LYON [France], 17-20 April 2005.

9 Mahato D N, Mathur B K & Bhattacherjee S , *J Mater Sci* Lett, 12 (1993) 1350.

10 Hoseman R & Bagchi S N, *Direct Analysis of Diffraction by Matter* (North Holland Publishing Co), 1962.

11 Vainshtein B K, *Diffraction of X-rays by Chain Molecules* (Elsevier Publishing Co, New York), 1966.

12 Alexander L E, *X-ray Diffraction Methods in Polym Sci* (Wiley-Interscience, New York), 1969.

13 Mitra G B & Mukherjee P S, *Polym*, 21 (1980) 1403.

14 Sarko A, *Wood and Cellulosics* (Ellis Horwood Ltd. Chichester), 1987, pp 55.

15 Li Z F & Netravali A N, *J Appl Polym Sci*, 44 (1992) 319.

16 Hon David N S, J *Appl Polym Sci*, 29 (1984) 2777.

17 Brigs D, *Practical Surface Analysis*, Briggs D & Seah M P Eds, (John Wiley & Sons), 1983, pp 359.

18 Clark D T, *Photon, Electron and Ion Probes of Polymer Structure and Properties*, Dwight D W, Falish T J & Thomas H R, Eds., ACS Symposium Series 162, Washington D C, 1981, pp 277.

19 Mahato D N, Mathur B K & Bhattacherjee S, *Indian J Phys,* 67A (1993) 251.

20 Mahato D N, PhD Thesis, *X-ray Structural Studies and Variation of Physical Properties of Coir Fiber with Alkali and Heat Treatments*, I I T Kharagpur, 1994.

21 Blackwell J, Vasko P D & Koening J L, *J Appl Phys*, 41 (1970) 4375.

22 Oltus E, *Cellulose Chem Technol*, 2 (1968) 311.

23 Liang C Y & Marshessault R H, *J Polym Sci*, 43 (1960) 71.

24 Liang C Y & Marchessault R H, *J Polym Sci,* 39 (1959) 269.

25 Revol J F & Goring D A, *J Appl Polym Sci,* 26 (1981) 1275.

26 Kolpak F J & Blackwell, *J Macromolecules*, 9 (1976) 273.